

# MECHANICAL PROPERTIES DETERMINATION BY REAL-TIME ULTRASONIC CHARACTERIZATION OF THERMALLY DAMAGED ENERGETIC MATERIALS

Alexander S. Tappan, Anita M. Renlund, Jeanne C. Stachowiak,  
Jill C. Miller and Michael S. Oliver  
Sandia National Laboratories\*  
Albuquerque, NM 87185

Understanding the physical properties of thermally-damaged energetic materials (EMs) in cookoff scenarios is vital to developing and validating predictive codes to describe ignition and post-ignition behavior. A small-scale experiment, called the “ultrasonic hot cell” is used to determine how certain physical properties of EMs change as thermal damage evolves. The experiment involves the controlled heating of a 6.35-mm-diameter cylindrical EM sample within rigid radial confinement. Moveable pistons provide axial confinement of the EM, which is measured by a load cell and LVDT extensometer and feedback-controlled by means of a pneumatic cylinder. Ultrasonic time-of-flight measurements were taken and combined with LVDT length measurements to measure the ultrasonic velocity as the EM decomposed. By combining data from shear and longitudinal ultrasonic experiments, the real-time elastic moduli of thermally-degraded HMX and PBX-9501 at three, constant axial force loads were determined. Higher loads caused higher ultrasonic velocities and moduli values. Decomposition resulted in decreasing moduli values for HMX, but relatively constant values for PBX-9501.

## INTRODUCTION

Thermal explosions of weapons and ordinance continue to present a serious threat to personnel and assets and therefore cookoff continues to be an important area of energetic material (EM) research. Research in this area has evolved further away from

large-scale tests and more towards model-based predictions based on heavily instrumented, small-scale experiments. Heavily instrumented experiments provide information on the physical and chemical changes in energetic materials during thermal damage evolution. Modeling relies on this EM experimental information along with additional information on boundary conditions to construct codes and models to predict EM behavior in extreme environments. Experimentation and simulation provide feedback between one another, and the results of one drive the

---

\*Sandia is a multiprogram laboratory operated by Sandia Corporation, a Lockheed Martin Company, for the United States Department of Energy under contract DE-AC04-94AL85000.

other forward. The philosophy behind this approach is that costly full-scale experiments can be reduced and material properties can be understood better by utilizing relatively small-scale experiments and computer models to predict the cookoff behavior of full-scale weapon systems.

The state of an energetic material at the time of cookoff depends on closely coupled chemical and physical phenomena. The fundamental damage mechanism is thermally-induced chemical decomposition, but the thermally-induced physical changes, which arise both independently and also directly from this chemical decomposition, are equally important. The damage state is manifested by changes such as void formation, gas formation, microstructural changes, density changes, phase transitions, cracks, porosity, gas pressurization, mechanical softening and/or stiffening, binder migration, hot spot formation, and formation of inhomogeneities. The damage state of the material at the time of ignition will define the degree of violence and will determine whether the subsequent reactive wave may undergo a deflagration-to-detonation transition.

A series of related small-scale experiments based on an apparatus called the “hot cell” have been utilized to understand the physical changes that occur in EMs as they are exposed to extreme thermal environments.<sup>1-3</sup> The hot cell is used to heat a small sample of energetic material, and by utilizing a variety of different diagnostics, properties such as volumetric expansion, pressurization, phase change, elastic moduli, temperature excursions, compaction, extrusion and porosity evolution are investigated. The work presented here is performed with a variation of the apparatus known as the “ultrasonic hot cell.”

## EXPERIMENTAL

The basic ultrasonic hot cell apparatus (Figure 1) has been described elsewhere.<sup>2</sup> Briefly, a  $6.35 \times 6.35$ -mm cylindrical EM pellet is radially confined within a stainless-steel cell. The pellet is confined axially by opposing, movable Invar (a low coefficient of thermal expansion steel) pistons, inserted into the cell. O-rings seal the cell and confine decomposition products. The cell is heated by a band heater, which is installed around the circumference of the cell. The apparatus is confined rigidly within a load frame and instrumented with thermocouples, a load cell, a linear variable differential transformer (LVDT) and ultrasonic transducers in acoustic contact with the ends of the pistons. The displacement (LVDT) and force (load cell) are both measured in the axial direction, that is, along the length of the explosive pellet, as there is little change in the radial direction due to heavy confinement. A pneumatic cylinder, installed at the top of the load frame, is feedback-controlled with respect to either the LVDT or load cell. If the feedback

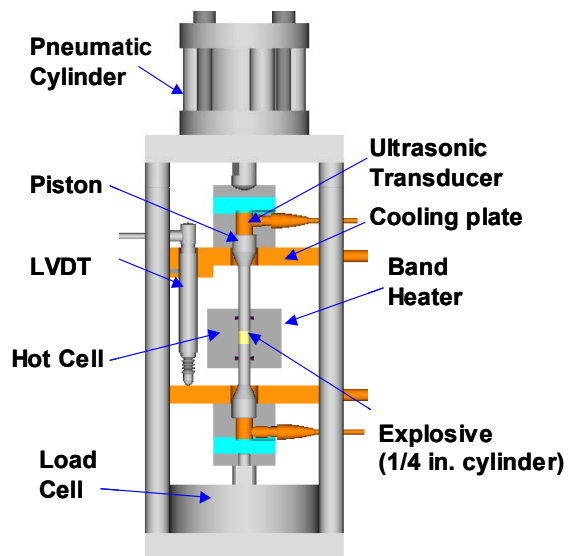


**FIGURE 1. ULTRASONIC HOT CELL APPARATUS.**

control is based on the LVDT measurement, the experiment is referred to as “displacement-controlled.” If the feedback control is based on the load cell measurement, the experiment is referred to as “load-controlled.” It is possible to switch back and forth between displacement and load control within the same experiment and also to perform controlled load and displacement cycles. The nitrogen supply to the pneumatic cylinder, and therefore, force to the pellet, is feedback-controlled by a mechanical testing system controller. Both the longitudinal and shear ultrasonic velocities were measured at 5.0 MHz. The ultrasonic waveforms are collected by a digital oscilloscope and transferred to a personal computer, which collects all data from the other diagnostics through a custom data acquisition program. Pulse-echoes (PEs) make up two of the waveforms and result from an ultrasonic wave reflection from the end of each piston in contact with the EM. A through-transmitted (TT) wave is generated when the excitation pulse of one transducer is received by the opposite transducer. If the travel times of the two PEs are  $t_1$  and  $t_2$ , and the TT travel time is  $t_3$ , then the time of flight through the sample is calculated by:

$$t = t_3 - (t_1 + t_2)/2. \quad (1)$$

The velocity through the sample is given by:

$$c_{L,S} = L / t, \quad (2)$$

where  $L$  is the length of the sample,  $c_L$  is the longitudinal sound speed and  $c_S$  is the shear sound speed.

A series of 12 experiments were conducted on HMX (1,3,5,7-tetranitro-1,3,5,7-tetraazacyclooctane) and PBX-9501 (95% HMX, 2.5% Estane, 2.5% BDNPA-F (bis(2,2-dinitropropyl) acetal/formal), a

nitroplasticizer) to examine the two materials’ behaviors during a thermal cycle. HMX was pressed at Sandia from bimodal powder as received from Holston Defense Corporation to a density of 1.82 g/cc. PBX-9501 pellets were machined from pressed material prepared at Los Alamos National Laboratory and had an average density of 1.83 g/cc. For each material, two experiments were performed at each constant load of 40, 120 or 240 lbs. (18, 54 or 110 kg), which for a 6.35-mm-diameter piston, corresponds to an axial force of 5.6, 17 or 34 MPa (820, 2500 or 4900 psi). The samples were heated according to a controlled temperature ramp that involved heating from room temperature to 40 °C, soaking at 40 °C for 15 min, heating to 190 °C at 7 °C/min and finally soaking at 190 °C for 100 min. This heating profile results in significant decomposition, but is conservative enough to not risk equipment damage due to cookoff. During this heating profile, displacement and ultrasonic data were collected every 10 seconds. For each load, two experiments were conducted, one utilizing longitudinal ultrasonic transducers and the other utilizing shear ultrasonic transducers. The combination of ultrasonic velocities from each pair of experiments allows calculation of the elastic moduli of the material based on the following relations:

$$\lambda = c_L^2 \rho - 2\mu \quad (3)$$

$$\mu = c_S^2 \rho \quad (4)$$

$$E = \mu(2\mu + 3\lambda)/(\lambda + \mu) \quad (5)$$

$$K = (3\lambda + 2\mu)/3 \quad (6)$$

$$\sigma = \lambda/2(\lambda + \mu), \quad (7)$$

where  $\lambda$  and  $\mu$  are the Lamé constants ( $\mu$  is also the shear modulus),  $c_L$  is the

longitudinal ultrasonic velocity,  $c_s$  is the shear ultrasonic velocity,  $\rho$  is the density at any given time during the experiment,  $E$  is Young's modulus,  $K$  is the bulk modulus, and  $\sigma$  is Poisson's ratio.<sup>4</sup> The material is treated as homogenous, isotropic and polycrystalline, in which directional effects are averaged due to orientational randomness.

## RESULTS AND DISCUSSION

Data from a typical experiment are presented in Figure 2. In this experiment, HMX was heated at a constant load of 17 MPa (120 lbs.), while the longitudinal ultrasonic velocity was measured. The sample length and ultrasonic velocity data on the figure have been normalized so they fill the entire scale of the graph. Prior to the HMX  $\beta$ - $\delta$  phase transition near 180 °C, the ultrasonic velocity increases, from 2.0 mm/ $\mu$ s to 2.8 mm/ $\mu$ s, with a concomitant increase in the pellet length, as measured by the LVDT. Because the load on the pellet is not allowed to change during the experiment, these two results lead to the conclusion that the initial thermal expansion of HMX into a confined volume causes an effective stiffening and therefore an increase in the sound velocity. Based on other experiments, this effect is more pronounced at higher loads, with higher loads causing a higher initial sound velocity and less of a change in the velocity from the heating from room temperature to the onset of the  $\beta$ - $\delta$  phase transition. Just prior to the phase transition, the pellet length change reaches a plateau, which is likely due to shrinkage, as observed in previous hot cell experiments,<sup>2</sup> and in agreement with X-ray diffraction and thermomechanical analysis of Herrmann et al.<sup>5-6</sup> During the phase transition, which occurs roughly 40 minutes into the experiment (over 178 °C to 188 °C), the ultrasonic velocity quickly decreases from

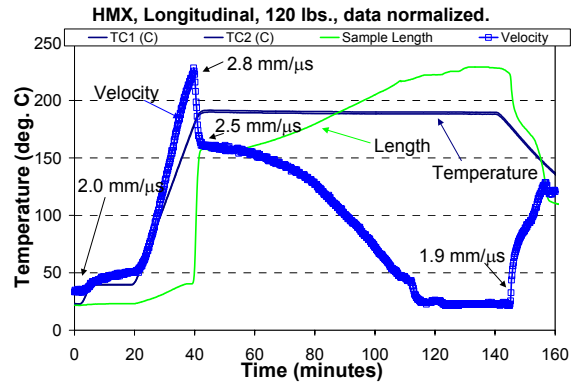


**FIGURE 2. LONGIDUDINAL ULTRASONIC VELOCITY AND PELLET LENGTH FOR A 17 MPa CONSTANT-LOAD HMX EXPERIMENT. DATA HAVE BEEN NORMALIZED.**

2.8 mm/ $\mu$ s to 2.5 mm/ $\mu$ s, with a concomitant increase in the pellet length. This increase indicates that  $\delta$ -HMX is less dense than  $\beta$ -HMX, in agreement with X-ray data,<sup>5-7</sup> and that the sound speed is less also, as one would expect with a lower density material of nearly identical structure. It is interesting that thermal expansion into a confined volume causes an initial increase in sound velocity, but during the phase transition, there is a decrease in the sound velocity, despite the even larger volumetric expansion. The phase transition in this experiment corresponds to a density change of 5.6%, somewhat less than the phase transition density change of 6.7% as measured by X-ray diffraction.<sup>6</sup> This difference is presumably due to expansion into ullage within the apparatus, incomplete phase transition, simultaneous grain compaction during phase transition, or some combination of these three phenomena. After the phase transition, the ultrasonic velocity continues to decrease from 2.5 mm/ $\mu$ s to a final value of 1.9 mm/ $\mu$ s at the end of the temperature soak, with a concomitant increase in the pellet length, presumably due to pressure exerted by

gaseous decomposition products. The decomposition of HMX likely decreases the sound velocity by simple mass conversion of the higher sound speed solid material to the lower sound speed gaseous material. Although not depicted in the figure, the attenuation of this sound wave increases during the bulk of this decomposition, supporting our previous observations of porosity evolution.<sup>8</sup>

Data from a similar experiment with PBX-9501 are shown in Figure 3. The experimental conditions are identical to the one presented above, except that the EM is PBX-9501. The velocities are somewhat higher than in pure HMX, except for the velocities at the end of the phase transition, where PBX-9501 is slightly lower. This is presumably due to the plastic binder being softest at this high temperature. The overall higher sound speeds are due to the 5% plastic binder content. The ultrasonic velocity trends during thermal decomposition are markedly different than that for pure HMX. Prior to the phase transition, during the initial heating ramp, the ultrasonic velocity decreases from 2.9 mm/μs to 2.6 mm/μs. This decrease is presumably due to softening of the binder as the PBX-9501 is heated, which is in agreement with the work of Funk et al.<sup>9</sup> This behavior is quite different from pure HMX, in which the ultrasonic velocity increases. Comparison of these responses of the two materials demonstrates that HMX and the binder exhibit competing effects on the sum ultrasonic response during the initial heating of PBX-9501, with the binder softening dominating during the initial heating. The HMX β to δ phase transition occurs roughly 40 minutes into the experiment (over 184 °C to 190 °C), which is a slightly higher temperature than that for HMX. During the phase transition, the ultrasonic velocity decreases further from

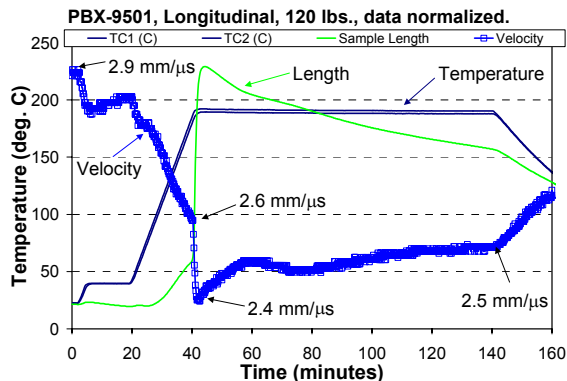


**FIGURE 3. LONGIDUDINAL ULTRASONIC VELOCITY AND PELLET LENGTH FOR A 17 MPa CONSTANT-LOAD PBX-9501 EXPERIMENT. DATA HAVE BEEN NORMALIZED.**

2.6 mm/μs to 2.4 mm/μs. This decrease coincides with the same decrease in pure HMX, but is slightly less pronounced. In both pure HMX and PBX-9501, the HMX dominates the acoustical response during the phase transition. Any changes that occur in the binder are masked by the greater change due to the phase transition. During the temperature soak at 190 °C, the ultrasonic velocity increases from 2.4 mm/μs to 2.5 mm/μs. During the temperature soak, the pellet length decreases, which indicates that the pellet is compacting. The increase in ultrasonic velocity is what would be expected with a compaction of the pellet. This result is not to say that the only effect is an increase in the density of the pellet. The compaction may be the result of the formation of voids due to decomposition, and a subsequent crushing of the voids. The fact that this is not seen in pure HMX suggests that another process may be responsible for the compaction. We have observed upon postmortem analysis of PBX-9501 samples, a viscous product in the void areas of the cell, especially in between the pistons and the inner walls of the cell. This viscous product was observed upon disassembly of the cell as a sticky, brown

fluid, coating the surfaces of the cell and pistons. This viscous product appeared to have extruded from the bulk of the pellet. High performance liquid chromatography and gel permeation chromatography analysis of this product from other hot cell experiments shows that it contains primarily nitroplasticizer and high molecular weight components, presumably Estane degradation products. The two potential acoustic effects of extrusion of this product are removal of a lower velocity component and compaction of the remaining material, both which contribute to an increase in ultrasonic velocity.

Longitudinal and shear ultrasonic velocities at three points within each of the twelve experiments are compiled in Table 1. The initial sound speed represents the pristine material. Due to the importance of the HMX  $\beta$ - $\delta$  phase transition, the velocities before and after the phase transition are also shown. The initial velocity tends to be higher for higher loads. This is due to improved inter-crystalline contact resulting from compaction of the pellet. This variation is less pronounced for PBX-9501 due to the already present, superior inter-crystalline contact, resulting from the presence of 5% binder. It should be noted that within the three measurements for each individual material, the three pre-transition ultrasonic velocities tend to be nearly equal. This is especially true of the longitudinal velocities. This is due to the thermal expansion of the pellets negating the differences in initial load and improving inter-crystalline contact through compaction.

The initial longitudinal ultrasonic velocity ranged from 1.87 – 2.27 mm/ $\mu$ s for HMX and 2.72 – 2.93 mm/ $\mu$ s for PBX-9501. The initial shear ultrasonic velocity ranged from 1.06 – 1.44 mm/ $\mu$ s for HMX and 1.07 – 1.54 mm/ $\mu$ s for PBX-9501. To

our knowledge, this is surprisingly the first report of the sound speed in pressed HMX samples, besides our previous work.<sup>2</sup> The results for PBX-9501 ( $c_L = 2.97$  mm/ $\mu$ s,  $c_S = 1.39$  mm/ $\mu$ s) have been reported and agree well with our higher-load data.<sup>10</sup> The initial pellet mass was approximately 360 mg, with mass loss over the course of the experiment ranging from 15 mg to 18 mg for PBX-9501 samples, and 10 mg to 15 mg for HMX samples. PBX-9501 samples apparently lose a greater fraction of their mass due to the combination of different reactivity, and decomposing binder migration out of the pellet, complicating measurement of the true final pellet mass.

The real-time bulk modulus results for HMX and PBX-9501 at the three different loads of 5.6, 17 and 34 MPa are shown in Figure 4. These results represent the changing bulk modulus of these materials as they are heated and eventually degrade. Each value can be thought of as the instantaneous bulk modulus of the material at that stage of degradation. Within the results from each material, there is little observable trend in the ordering of bulk moduli by load, except for HMX in the region before and after the  $\beta$ - $\delta$  phase transition in which higher values of the bulk modulus are measured at higher loads. Overall, the bulk modulus of PBX-9501 is higher than the bulk modulus of HMX. The only exception to this is during the phase transition, during which the values overlap to some extent. This is also observed when examining the ultrasonic velocities. During the initial heating cycle, the bulk modulus of HMX increases. This is due to the thermal expansion of the material into confinement, causing an effective stiffening, which causes a similar trend in the ultrasonic velocity. The bulk modulus of PBX-9501 decreases during the initial heating, despite the observed increase in pure HMX during this

**TABLE 1. LONGITUDINAL AND SHEAR ULTRASONIC VELOCITIES AT THREE POINTS WITHIN EACH OF THE TWELVE EXPERIMENTS.**

Longitudinal Ultrasonic Velocity (mm/ $\mu$ s)						
	HMX			PBX-9501		
Position on Heating cycle	5.6 MPa (40 lbs.)	17 MPa (120 lbs.)	34 MPa (240 lbs.)	5.6 MPa (40 lbs.)	17 MPa (120 lbs.)	34 MPa (240 lbs.)
Initial	1.87	1.98	2.27	2.72	2.90	2.93
Pre-transition	2.70	2.82	2.82	2.59	2.57	2.55
Post-transition	2.62	2.53	2.47	2.48	2.40	2.39
Shear Ultrasonic Velocity (mm/ $\mu$ s)						
	HMX			PBX-9501		
Position on Heating cycle	5.6 MPa (40 lbs.)	17 MPa (120 lbs.)	34 MPa (240 lbs.)	5.6 MPa (40 lbs.)	17 MPa (120 lbs.)	34 MPa (240 lbs.)
Initial	1.06	1.28	1.44	1.07	1.47	1.54
Pre-transition	1.53	1.62	1.69	1.02	1.32	1.31
Post-transition	1.42	1.38	1.49	0.96	1.14	1.19

period. As with the ultrasonic velocities, this demonstrates that the HMX and binder exhibit competing phenomena, with the

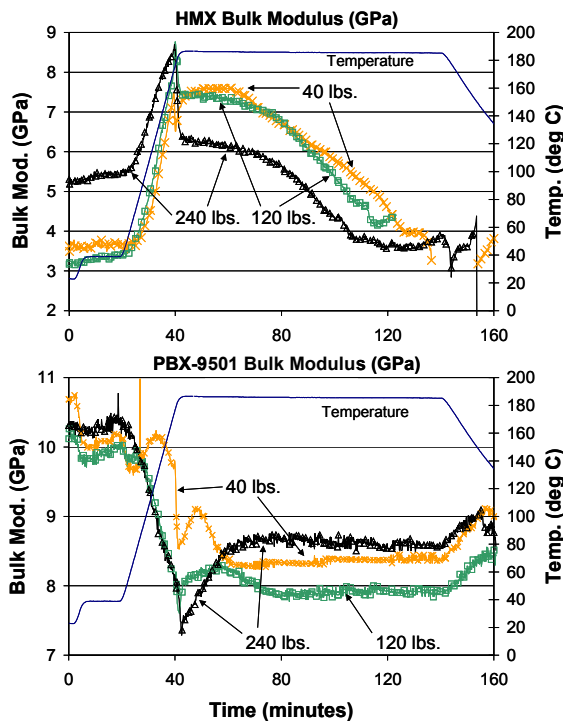


**FIGURE 4. REAL-TIME BULK MODULUS FOR 17-MPa CONSTANT-LOAD HMX AND PBX-9501 EXPERIMENTS.**

softening of the binder dominating during the initial heating cycle. Thus, the softening of binder has a greater contribution than the thermal expansion of the HMX to the value of both the ultrasonic velocity and the bulk modulus. During the phase transition, which occurs 40 minutes into the experiment, the bulk modulus decreases for both HMX and PBX-9501. This is an indication that  $\delta$ -HMX is a softer material than  $\beta$ -HMX and that the binder in PBX-9501 plays little role in the bulk modulus changes during the phase transition. The competing effects of HMX and the binder, seen during the initial heating, are both overwhelmed by the softening during the phase transition. After the phase transition and during the final 190 °C soak, the two materials again behave very differently. HMX shows an accelerating decrease in the bulk modulus as the material degrades, presumably due to porosity evolution from decomposition. The acceleration may be an indication of increasing decomposition rate. The bulk modulus of PBX-9501 stays relatively constant during this soak. This contrast in the two materials' behaviors may be the result of extrusion of a viscous product from

the PBX-9501 pellet and compaction of the remaining material, which is obviously not possible in pure HMX. The steady extrusion of this fluid (softer component) away from the bulk of the sample (stiffer component) may compensate for the bulk modulus decrease observed during degradation of pure HMX. The extrusion of this material would most definitely introduce error into

the PBX-9501 measurements, although this error was not quantified.

Table 2 shows a summary of Young's modulus, the shear modulus, the bulk modulus and Poisson's ratio for the two materials, at four points within each experiment pair for the three load conditions. The values for the pristine

**TABLE 2. YOUNG'S MODULUS, THE SHEAR MODULUS, THE BULK MODULUS AND POISSON'S RATIO FOR THE TWO MATERIALS, AT FOUR POINTS WITHIN EACH EXPERIMENT PAIR FOR THE THREE LOAD CONDITIONS.**

Material, Load	Position on Heating cycle	Young's Modulus (GPa)	Shear Modulus (GPa)	Bulk Modulus (GPa)	Poisson's Ratio (dimensionless)
HMX 5.6 MPa (40 lbs.)	Initial	5.3	2.0	3.7	0.27
	Pre-transition	10.5	4.2	7.5	0.27
	Post-transition	8.9	3.4	6.5	0.30
	End of hold	6.8	2.9	3.4	0.20
HMX 17 MPa (120 lbs.)	Initial	6.9	3.0	3.2	0.14
	Pre-transition	12.0	4.8	8.6	0.24
	Post-transition	9.4	3.7	7.5	0.29
	End of hold	N/A <sup>a</sup>	N/A <sup>a</sup>	N/A <sup>a</sup>	N/A <sup>a</sup>
HMX 34 MPa (240 lbs.)	Initial	9.1	3.8	5.2	0.21
	Pre-transition	13.0	5.2	8.8	0.26
	Post-transition	9.8	3.8	7.7	0.29
	End of hold	6.9	2.6	5.2	0.26
PBX-9501 5.6 MPa (40 lbs.)	Initial	5.9	2.1	10.7	0.41
	Pre-transition	5.2	1.8	9.8	0.42
	Post-transition	4.5	1.6	8.6	0.41
	End of hold	4.9	1.7	8.4	0.40
PBX-9501 17 MPa (120 lbs.)	Initial	10.3	3.9	10.1	0.33
	Pre-transition	8.3	3.1	8.1	0.33
	Post-transition	6.7	2.5	7.7	0.36
	End of hold	8.2	3.1	7.9	0.32
PBX-9501 34 MPa (240 lbs.)	Initial	11.4	4.3	10.3	0.32
	Pre-transition	8.4	3.2	8.1	0.32
	Post-transition	7.3	2.7	7.4	0.34
	End of hold	9.8	3.8	8.4	0.31

<sup>a</sup> Due to difficulties tracking the shear ultrasonic wave, these values were not calculated late in the experiment.

material, the material before and after the HMX  $\beta$ - $\delta$  phase transition and the material at the end of the 100-minute temperature soak at 190 °C are reported. These values were calculated from the longitudinal and shear velocities and an estimation of the density of the pellet, based on the LVDT pellet length measurement and assuming no mass loss. With each of the three moduli reported, the value decreases during the phase transition, indicating that  $\delta$ -HMX is a softer material than  $\beta$ -HMX. Other values of bulk modulus for pristine  $\beta$ -HMX have been determined. Experimental values include: 13.6 GPa,<sup>11</sup> 11.67-12.51 GPa,<sup>12</sup> and 12.4 GPa.<sup>13</sup> Calculated values include: 14.53 and 16.86 GPa,<sup>14</sup> and 10.2 and 12.5 GPa.<sup>15</sup> All of our reported values are lower than these previously reported values. The discrepancy is likely due to the fact that the above values were derived from experiments on one or a few single crystals, or calculations on few-molecule ensembles, whereas our values are measured from a bulk sample. This being the case, our measurements reflect bulk properties associated with inter-crystalline contact.

## SUMMARY AND CONCLUSIONS

The real-time shear and longitudinal ultrasonic velocities, Young's modulus, the shear modulus, the bulk modulus and Poisson's ratio of HMX and PBX-9501 have been measured at three constant loads, during a heating cycle. The changes in elastic moduli of HMX and PBX-9501 show that  $\delta$ -HMX is a softer material than  $\beta$ -HMX. During a temperature soak of 190 °C, HMX showed an increase in pellet length, while PBX-9501 showed a decrease. The ultrasonic velocity measurements tended to equilibrate just prior to the phase transition. During the phase transition, both the shear and longitudinal velocities decreased for both HMX and PBX-9501.

During the temperature soak at 190 °C, the bulk modulus of HMX decreased due to decomposition, whereas the bulk modulus of PBX-9501 stayed relatively constant, despite decomposition. These differing results are presumably due to the extrusion of a softer component out of the degrading PBX-9501, with subsequent compaction of the remaining material. This so called "viscous product" was analyzed from other experiments and found to be composed of primarily nitroplasticizer and high molecular weight components, presumably Estane degradation products.

## ACKNOWLEDGEMENTS

The authors wish to thank Deanne Idar of LANL for supplying the PBX-9501 used in this study. The authors cannot thank John H. Gieske (ret. Sandia) enough for his preliminary work on this system and expert knowledge of ultrasonic measurements. This work was supported by Sandia's Engineering Sciences Research Foundation and the Memorandum of Understanding under the Technical Coordinating Group for Energetic Materials (TCG-III).

## REFERENCES

1. Renlund, A.M., Kaneshige, M.J., Schmitt, R.G. and Wellman, G.W., "Mechanical Response and Decomposition of Thermally Degraded Energetic Materials: Experiments and Model Simulations," 1999 JANNAF Propulsion Systems Hazards Subcommittee Meeting, Cocoa Beach, FL (18-22 Oct 1999).
2. Tappan, A. S., Renlund, A. M., Miller, J.C., Casstevens, J.C. and Oliver, M.S., "Real-Time Ultrasonic Characterization of Thermally-Damaged Energetic Materials Approaching Cookoff," 2002 JANNAF

Propulsion Systems Hazards Subcommittee Meeting, Destin, FL (8-12 April 2002).

3. Kaneshige, M.J., Renlund, A.M., and Schmitt, R.G., "Mechanical Response of Heated PBXN-109," 2000 JANNAF Propulsion Systems Hazards Subcommittee Meeting, Monterey, CA (13-17 Nov 2000).

4. Huntington, H. B., The Elastic Constants of Crystals (New York: Academic Press, 1958) 9-10.

5. Herrmann, M., Engel, W. and Eisenreich, N., "Thermal analysis of the phases of HMX using X-ray diffraction," *Zeitschrift für Kristallographie*, 204, 121-128, (1993).

6. Herrmann, M., Engel, W., and Eisenreich, N. "Thermal Expansion, Transitions, Sensitivities and Burning Rates of HMX," *Propellants, Explosives, Pyrotechnics*, 17, 190-195, (1992).

7. Cady, H.H., Larson, A.C., Cromer, D.T., "The Crystal Structure of  $\alpha$ -HMX and a Refinement of the Structure of  $\beta$ -HMX," *Acta Crystallographica*, 16, 617-623, (1963).

8. Renlund, A.M., Miller J.C., Trott, W.M., Erickson, K.L., Hobbs, M.L., Schmitt, R.G., Wellman, G.W. and Baer, M.R. "Characterization of Thermally Degraded Energetic Materials," 11th Symposium (International) on Detonation. Snowmass, CO (Aug. 31-Sept. 4, 1998).

9. Funk, D.J.; Laabs, G.W.; Peterson, P.D.; Asay, B.W., "Measurement of the stress/strain response of energetic materials as a function of strain rate and temperature: PBX 9501 and Mock 9501," American Physical Society Biennial Conference on Shock Compression of Condensed Matter, Seattle, WA (13-18 Aug 1995).

10. Olinger, B. in: Morris, C.E., ed., Los Alamos Shock Wave Profile Data (Berkeley, Los Angeles, London: University of California Press, 1982) 280.

11. Olinger, B, Roof, B. and Cady, H., in *Actes du Symposium International sur le Comportment des Milieux Denses Sous Hautes Pressions Dynamiques*; Editions du Commissariat al'Energie Atomique, Centre d'Etudes Nucleaires de Sarclay: Paris (1978) 3.

12. Zaug, J.M., "Elastic Constants of  $\beta$ -HMX and Tantalum, Equations of State of Supercritical Fluids and fluid Mixtures and Thermal Transport Determinations," 11th Symposium (International) on Detonation. Snowmass, CO (Aug. 31-Sept. 4, 1998).

13. Yoo, C.S. and Cynn, H., "Equation of State, Phase Transition, Decomposition of  $\beta$ -HMX (octahydro-1,3,5,7-tetranitro-1,3,5,7-tetrazocine) at High Pressures," *Journal of Chemical Physics*, 111, 10229-35 (1999).

14. Sorescu, D. C., Rice, B. M., and Thompson, D. L., "Theoretical Studies of the Hydrostatic Compression of RDX, HMX, HNIW and PETN Crystals," *Journal of Physical Chemistry B*, 103, 6783-6790, (1999).

15. Lewis, J. P., Sewell, T. D., Evans, R. B., and Voth, G. A., "Electronic Structure Calculation of the Structures and Energies of the Three Pure Polymorphic Forms of Crystalline HMX," *Journal of Physical Chemistry B*, 104, 1009-1013, (2000).